

An Investigation of Spatially Dependent Atmospheric Refractivity Characteristics within Atmospheric Rivers and their Importance for Airborne Radio Occultation Observations

Janelle Wargo

Jennifer S. Haase, Michael J. Murphy, Bing Cao

Introduction & Background

Atmospheric rivers (ARs) are narrow, low-altitude corridors of strong horizontal water vapor transport which occur over mid latitude regions. Recently ARs have been split into 5 regions - a core, cold, warm, non-AR cold, and non-AR warm sector.<sup>1</sup> These regions are defined by their integrated vapor transport (IVT) levels, a metric based on specific humidity multiplied by the horizontal wind vector integrated over pressure levels. This summer, however, was focused on sectioning an AR based on its entire vertical profile in order to not overlook the different components that exist in an AR’s vertical cross-section, as seen in Figure 1.

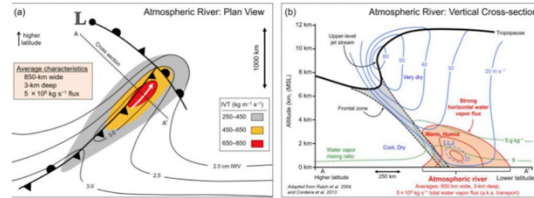


Figure 1. 2017, Ralph et al., Journal of Hydrometeorology, “Dropsonde Observations of Total Integrated Water Vapor Transport within North Pacific Atmospheric Rivers”

Additionally, Global Navigation Satellite System (GNSS) Airborne Radio Occultation (ARO) data was investigated. ARO is a technique of remote sensing where radio waves emitted from a GNSS satellite orbiting the Earth reach a Septentrio Asterxu phase tracking receiver on an AR Reconnaissance (Recon) flight. By using the climatology profile in conjunction with a raytracing algorithm the excess time that it took for the wave to reach the receiver is calculated. Using this the bending angle - the angle at which the wave bent through the atmosphere based on the refractive index - is found. Next, using an Abel inversion the actual refractivity profile of the atmosphere can be calculated. This retrieved refractivity profile is extremely relevant due to the fact that refractivity is based on temperature (T), pressure (P), and water vapor partial pressure (e) as seen in Equation 1.

$$(1) N = (n - 1) * 10^6 = \frac{77.6890P}{T} - \frac{6.3938e}{T} + \frac{3.75463 * 10^5 e}{T^2}$$

Thus, calculating a refractive profile is important to AR forecasting and modelling. In previous studies, it has also been clear that some refractive profiles seem to be similar to others across an AR<sup>2</sup>, continuing the question of whether ARs can be split into sectors based on the vertical refractivity profiles. It is also important to note that large amounts of ARO data are discarded during processing due to signal loss while in the presence of sharp vertical gradients of refractivity. This results in certain profiles being truncated, rendering them unusable for forecasting and modelling.

Objectives & Methods

Thus, the overall research question was exploring whether the large dataset of observed profiles of refractivity gathered during AR Recon can be categorized in useful ways using machine learning. The objectives were to compute refractivity profiles from in-situ dropsonde observations and ARO data, to use machine learning to categorize refractivity profiles, relate these categories to the physical characteristics of ARs, and to develop the ability to place any given refractivity profile into its proper sector of an AR.

To accomplish this, data from 29 Intensive Observing Periods (IOPs) from AR Recon 2021 NOAA G-IV flights were used. Additionally, the decision to use k-means clustering machine learning was made; k-means clustering is an iterative process of partitioning observations into centroid-based clusters. This algorithm was first carried out using the in-situ dropsonde observations from IOP17 due to the fact that dropsondes provide observed profiles down to the Earth’s surface (they do not have the same issues that ARO has). These initial clusters were extremely promising to see - visually it was clear that there were different types of refractivity profiles across an AR; it was also decided to use 6 clusters as a way to both minimize variance and maintain visual organization.

<sup>1</sup> 2021, Cobb, Monthly Weather Review, “Atmospheric River Sectors: Definition and Characteristics Observed Using Dropsondes from 2014-20 CalWater and AR Recon”

<sup>2</sup> Murphy, et al., Depth of Penetration of GNSS RO in atmospheric rivers, in prep, MWR.

## Results

Next, the full dropsonde dataset from AR Recon 2021, which consisted of 425 observations, was analyzed. The k-means clustering results are shown in Figure 2. Figure 3 shows each refractive profile in the assigned cluster; Figure 4 shows the median cluster profile.

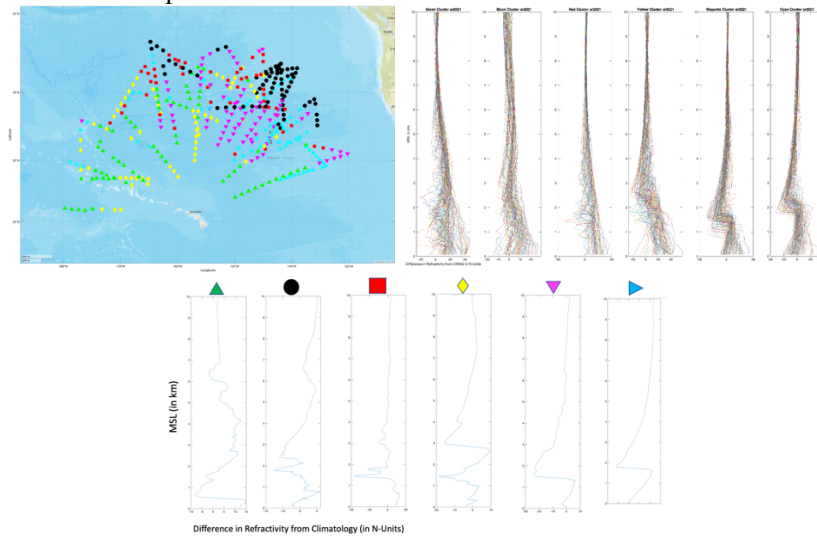


Figure 2. All NOAA-GIV flights AR Recon 2021 with color-coded clusters, Figure 3. Refractivity profiles of each cluster (AR Recon 2021). Each line represents a dropsonde profile, Figure 4. Dropsonde profile refractivity profile closest to each cluster's median.

From these profiles, it was possible to notice some key characteristics and patterns. To support these initial theories however, the median clusters' Skew-T Lop-P plots were analyzed in conjunction with the IVT values from the ERA5 reanalysis to deduce where in the AR each cluster belongs (Figure 5). From these plots and their location in respect to the ARs, the green cluster consists of tropical moisture export; the black cluster is the tail of the AR; the red cluster consists of the midlatitude core of AR and partial tail profiles; the yellow cluster is the warm side after the AR is present and tropical moisture export; the magenta and blue profiles are non-AR.

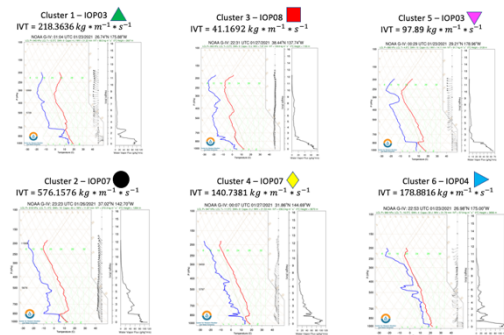


Figure 5. The closest to median dropsonde profile IVT and Skew-T plot.

Given this new knowledge of the centroid-based refractive profile clusters and their locations across an AR, ARO profiles were then evaluated. First, a deep penetrating refractive profile from a g15r satellite for IOP07 was chosen; this profile reaches from 10.0 km to 1.6 km above the Earth's surface. This depth meant that the profile has large amounts of viable data to be used. Using a script this profile was assigned to Cluster 6 - the non-AR side. The lack of moisture on the non-AR side means that the GNSS signals were able to penetrate very low. This output is seen in Figure 6. Next, a shallow penetrating profile (10.0 km to 8.3 km) was assigned to Cluster 3, a midlatitude core of AR/Tail (Figure 7). This is likely due to the high moisture content of the low-level jet in the core of an AR as seen in Figure 1; satellite signals are lost when they try to pass through this highly refractive environment.

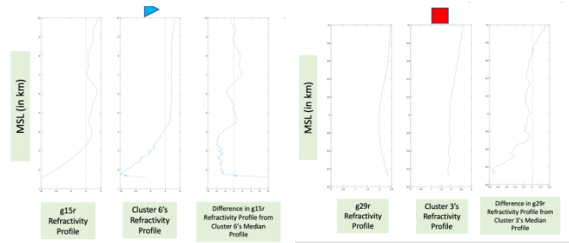


Figure 6. Plots output by script which assigned a deep penetrating profile to Cluster 6 (g15r, IOP07), Figure 7. Plots output by script which assigned a shallow penetrating profile to Cluster 3 (g29r, IOP07).

Based on these results, the rest of the ARO profiles from IOP07 were assigned to clusters. A plot of this is seen in Figure 8.

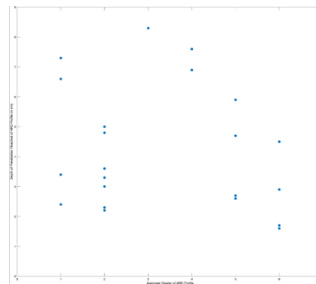


Figure 8. Depth of ARO profile penetration vs. the assigned cluster of the profile.

### Conclusion & Future Work

Based off this research, it is clear that k-means clustering can be helpful in discerning different sectors of ARs. It is evident that refractivity profiles change depending on the location in/around the AR – this is due to vertical characteristics. ARO profiles can then be assigned to these clusters. However, k-means appears to cluster all of the tropical moisture export together; in the future it would be important to include AF C-130 flights in the clustering and to try out more clusters in order to differentiate the profiles more. This would allow for more informed assignment of observation errors for the future. Additionally, it would help assist in adapting more advanced signal tracking techniques for ARO technology based on the specific atmospheric environment.

### Acknowledgements:

Anna M. Wilson, CW3E, Scripps Institute of Oceanography  
 CW3E: Marty Ralph, Director, Luca Delle Monache, Deputy Director  
 CW3E Summer Internship Program, Cody Poulsen